Journal of Non-Crystalline Solids 475 (2017) 10–14

Contents lists available at ScienceDirect

Journal of Non-Crystalline Solids

journal homepage: www.elsevier.com/locate/jnoncrysol

# Detailed structure of a new bioactive glass composition for the design of bone repair materials

Ailing Li[a], Huihui Ren[a,b], Yang Cui[a,b], Chao Wang[a,b], Xiaojuan Zhou[c], He Lin[c,*], Dong Qiu[a,*]

[a] Beijing National Laboratory for Molecular Sciences, State Key Laboratory of Polymer Physics and Chemistry, Institute of Chemistry, Chinese Academy of Sciences, Beijing 100190, China
[b] University of Chinese Academy of Sciences, Beijing 100190, China
[c] Shanghai Institute of Applied Physics, Chinese Academy of Sciences, Shanghai 201204, China

ARTICLE INFO

*Keywords:*
Structural characterization
Bioactive glass
Sol-gel
Phosphosilicate

ABSTRACT

Detailed structure of a new bioactive glass composition (PSC, 54 mol% $SiO_2$, 35 mol% CaO and 11 mol% $P_2O_5$) was studied, and conventional glasses (45S5 and S70C30) were used as comparison. The structure information were obtained by HEXRD and solid NMR techniques. It was found that all the samples have different silicon and phosphorous coordination environment, there is Si-O-P network formed for PSC samples but not for 45S5 and S70C30 samples. These results may hopefully advance the design of new bioactive glasses.

## 1. Introduction

The life expectancy of the world population increased dramatically every year because of the developments of people's life. Plenty of bone implants are needed to maintain their quality of life after accidents or illnesses. However, current implants, *e.g.* metals and polymers, were biological inert triggering fibrous encapsulation after implantation and leading to a high rate of failure in the long time [1]. In order to avoid the flaw of bone implants, material scientists have been making great effort to develop synthetic bone materials. Among them, bioactive glasses (silicate-based glasses, phosphate-based glasses, borate-based glasses and borosilicate glasses) have provided many encouraging results [2–7].

The first silicate-based bioactive glass (Bioglass®) were reported by Hench, which has a composition known as 45S5 corresponding to 45 wt %, $SiO_2$, 24.5 wt%, $Na_2O$, 24.5 wt% CaO, and 6 wt% $P_2O_5$, and has been widely used in clinical, *e.g.* dental and orthopaedic fields [8,9]. However, these glasses need to be processed at very high temperatures. Sol-gel bioactive glasses processed at lower temperature were then explored. It was found that the gel-derived glasses had high surface area, porosity, and wider range of bioactive compositions (58S, 77S and S70C30, et al.), exhibiting higher bone bonding rates [10]. However, all these silicate-based glasses degrade slowly and usually take 1 to 2 years to disappear from the body [11].

Phosphate-based glasses ($CaO\text{-}Na_2O\text{-}P_2O_5$) have unique dissolution properties in body fluids, the degradation rates can be controlled from hours to several weeks by changing the glass composition. Furthermore, these glasses can be synthesized as particles, fibres and microtubes to include different dopants that are able to induce a specific biological function and enhance biocompatibility in soft tissue [3]. However, these glasses didn't not embody good bioactivity for bone regeneration. Because of these limitations, it is necessary to search for new bioactive glasses compositions for the repair of bone defects.

Since the silicate-based glasses with lower phosphate content (< 5 mol%) have higher bioactivity for bone defects, whereas phosphate glasses without silicate content have higher degradation rates, it may be possible to prepare a new phosphosilicate bioactive glass with higher phosphate content accelerating the degradation rates for bone defects. In previously, we used a non-toxic phytic acid as phosphorous precursor to prepare $CaO\text{-}SiO_2\text{-}P_2O_5$ glasses by sol-gel process, it was found that a much broader range of bioactive composition were obtained especially at high phosphate content [12]. In which, the composition of $(CaO)_{0.35}(SiO_2)_{0.54}(P_2O_5)_{0.11}$ (48.2 wt% $SiO_2$, 29.1 wt% CaO and 22.7 wt% $P_2O_5$, termed as PSC) has the best bioactivity, and the phosphate content is dramatically increased compared with conventional bioactive glasses. The PSC have also be found to have better cell proliferation, mRNA expression and osteocalcin and mineralization of hDPCs comparing with conventional 45S5 [13], and the released Si and P ions from PSC were larger than those released from 45S5, implying the higher degradation rate for PSC.

Detailed structural knowledge is a prerequisite for optimizing glasses design. The atomic-scale structure of bioactive glasses and its effect on bioactivity and chemical durability has attracted much attention, because of which is important to model and predict the

* Corresponding authors.
*E-mail addresses:* linhe@sinap.ac.cn (H. Lin), dqiu@iccas.ac.cn (D. Qiu).

http://dx.doi.org/10.1016/j.jnoncrysol.2017.07.027
Received 10 May 2017; Received in revised form 7 July 2017; Accepted 27 July 2017
Available online 05 September 2017
0022-3093/ 

behavior of bioactive glasses, and ultimately improve their design [14–17]. In this paper, the detailed structure of this new bioactive glass composition (PSC) with higher phosphate content was studied by HEXRD and NMR techniques, which are possible to gain detailed insight into its structure. The linking between phosphate and silicate structural units will be answered, hopefully advancing the design of new bioactive glasses.

## 2. Experimental

### 2.1. Sample preparation

Tetraethyl orthosilicate (TEOS, ≥ 99.0%) and $Ca(NO_3)_2{\cdot}4H_2O$ were purchased from Sinopharm Chemical Reagent Co., Ltd. Phytic acid (50 wt% aqueous solution) was purchased from Sigma Aldrich. All the precursors were used without further purification in the sol-gel preparation.

Bioactive glass (PSC: $SiO_2$-54 mol%, CaO-35 mol%, $P_2O_5$-11 mol%) was prepared as previously reported [12]. Phytic acid (1.6 mL) was firstly added in the mixture of ethanol and water at room temperature, then TEOS (5.82 mL) was added through a syringe during stirring. After 1 h, $Ca(NO_3)_2{\cdot}4H_2O$ powder (3.98 g) was added until a transparent solution formed (the sol), which was sealed in polypropylene containers and left to gel. The resultant gel was aged at 60 °C for one week and then at 120 °C for another two weeks, and then stabilized at 200 °C, 400 °C and 600 °C for 1 h to get PSC glasses. The stabilized PSC glasses were then grounded into powders for testing.

Bioactive glasses 45S5 (Bioglas®:$SiO_2$-46.1 mol%,CaO-26.9 mol%, $P_2O_5$-2.6 mol%, $Na_2O$-24.4 mol%) and S70C30($SiO_2$-70 mol%, CaO-30 mol%), which have little or no phosphate content, were used as comparison. 45S5 glass was purchased from Schott. Bioactive glass S70C30 was prepared as previously reported [18]: TEOS (20 mL) was hydrolyzed in the mixture of ethanol and water for 30 min at room temperature with 2 N $HNO_3$ as catalyst. $Ca(NO_3)_2{\cdot}4H_2O$ (9.06 g) was added gradually under continuous stirring. The molar ratio of water to TEOS was 12:1. The obtained clear sol solution was sealed in a polypropylene container and left to gel. The gel was aged at 60 °C for a week, followed by drying at 120 °C for another week and then stabilized at 600 °C for 1 h to obtain the S70C30 glass. The stabilized S70C30 glasses were then grounded into powders for testing.

### 2.2. Thermogravimetric analysis (TGA-DSC)

Thermal gravimetric behaviors of the PSC gels were measured on a TA Q-600 instrument. The samples (around 5 mg each) were placed in alumina crucibles and measured under nitrogen flow at 20 mL·min$^{-1}$. Data were collected from 50 °C to 800 °C at a heating rate of 5 °C·min$^{-1}$.

### 2.3. X-ray diffraction (XRD)

XRD measurements were performed on a Rigaku (D/MAX 2500) instrument with Cu Ka radiation (λ = 1.54 Å), operated at 40 kV and 200 mA. The data were collected for 2θ values between 5 and 70° with a step size of 0.02°.

### 2.4. Fourier transform infrared spectroscopy(FTIR)

FTIR were collected in the range 4000–400 cm$^{-1}$ on a Bruker Einox 55 instrument. All samples were diluted with dry KBr, ground down to fine powders and pressed into pellets. Measurements were made at ambient temperature.

### 2.5. Bioactivity test and dissolution profile measurement

150 mg of PSC glass powders were immersed in 100 mL SBF at 36.5 ± 0.5 °C [19–22]; each sample was measured in triplicate. After immersing in SBF for 1 d, the powders were washed gently with pure water and left to dry in a desiccator without heating. Apatite formation was evaluated using FTIR and XRD.

### 2.6. Textural characterization

Pore texture of the PSC, S70C30 and 45S5 glass powders were analyzed using ASAP 2020 apparatus. The samples were degassed in vacuum oven at 200 °C for 10 h for the removal of moisture from the pores and then analyzed with nitrogen adsorption to determine the BET specific surface area (SSA).

### 2.7. Higher energy X-ray diffraction (HEXRD)

The atomic structure of the PSC, 45S5 and S70C30 glasses were characterized by HEXRD. The data were collected on BL13W1 in Shanghai Synchrotron Radiation Facility. The finely powdered glasses were enclosed inside a 2 mm thick circular metal annulus sealed on both sides by kapton film and mounted onto a flat-plate "θ:2θ" instrumental set-up. X-ray energy is 69.525 keV (λ = 0.1783 Å). The data was normalized against the incident beam intensity and corrected for the background scattering using the empty cell, and for sample absorption, polarization of the incident beam, inelasticity (Compton scattering), scattering volume and sample self-scattering. The resulting structure factor, S(Q), is Fourier transformed to obtain the total correlation function, T(r), in real space [23,24]. Structural information was obtained from the diffraction data by modelling the r-space data using NXFIT software to compare with the experimental total correlation function. The structural parameters used to generate the r-space simulation are varied to optimize the fit to the experimental data. The uncertainties of HEXRD fitting data arise mainly from the fitting process and the overlapping pair correlation shells.

### 2.8. Solid state NMR

The magic angle spinning (MAS) solid state Nuclear Magnetic Resonance (NMR) measurements of 45S5, S70C30 and PSC powders were carried out by an AVANCE III 400 MHz instrument providing $^{31}P$ and $^{29}Si$ Larmor frequency of 161.58 MHz and 79.3 MHz, respectively. 4 mm MAS BB probes spinning at 12 kHz were used. For $^{31}P$ NMR, a 2 μs (~90° tip angle) pulse was used, and the recycle delay was 1 s. For $^{29}Si$ NMR, a 2.0 μs pulse (~90° tip angle) was used, and the recycle delay was 2 s. $^{31}P$ and $^{29}Si$ NMR spectra were referenced using $NH_4H_2PO_4$ ($\delta_P$ = 0.9 ppm with respect to phosphoric acid) and tetramethylsilane ($\delta_{Si}$ = 0 ppm), respectively.

## 3. Results

### 3.1. TGA-DSC analysis

Fig. 1 shows TGA-DSC traces of representative PSC gels after dried at 120 °C. Three stages of weight loss are observed: the first one occur between 180 °C and 200 °C with an exothermic peak, which may be associated with the removal of trapped solvent (water, ethanol and nitrate *etc.*); the second one occur between 200 °C and 400 °C, which may because the further removal of nitrate and the loss of organic moieties by further condensation; the third stage of weight loss commence from the end of second weight loss (~400 °C) up to ~600 °C, which is most likely due to the further loss of organic moieties. In general, the dried gels show weight losses around 30% over the temperature range 50–800 °C during the course of TGA-DSC measurements. The end temperature of every stage is chosen as stabilization temperature for PSC glass, *i.e.* 200 °C, 400 °C and 600 °C.

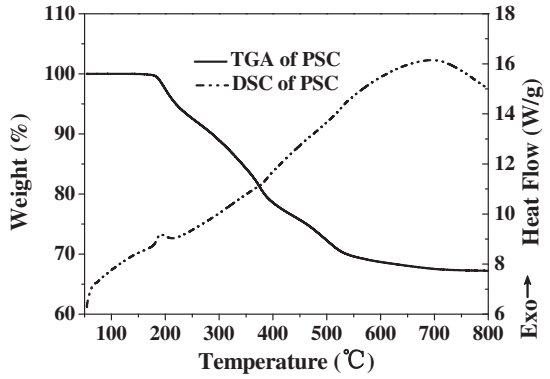


**Fig. 1.** The TGA-DSC traces of the calcium phosphosilicate gels (PSC: $(CaO)_{0.35}(SiO_2)_{0.54}(P_2O_5)_{0.11}$) after dried at 120 °C.

### 3.2. XRD spectra

Whether calcium is incorporated into the sol-gel glass network as a network modifier, has been the source of contention. In previous study, it had been reported that calcium nitrate crystals exist in dried gels unless stabilized at a temperature higher than 450 °C [25]. The PSC glasses were stabilized at different temperatures (200 °C, 400 °C and 600 °C) and test by XRD to indentify whether calcium nitrate crystals is existent, as shown in Fig. 2. It is found that all the glasses are amorphous and have no calcium nitrate crystal appeared. This means that calcium ions is incorporated into the network even at low temperature (200 °C), which may because that the phytic acid used as phosphorous precursor for PSC glass have high affinity with calcium ions, thus leading to the break down of calcium nitrate at lower temperature [16].

### 3.3. FTIR spectra

Calcium nitrate has been widely used as calcium precursor in sol-gel glass because of which is highly soluble, low cost and less thermal stable compared with other inorganic calcium salts, however, the remained nitrate ions have potentially toxicity [18]. Therefore stabilization process is needed for the removal of nitrate ions. The PSC glasses after stabilized at different temperatures (200 °C, 400 °C and 600 °C) were test by FTIR to see whether nitrate ions are removed, as shown in Fig. 3. It is found that the nitrate ions decreased dramatically with the increase of stabilization temperature, and the nitrate ions could be removed fully after stabilized at 600 °C. Thus all the following PSC glasses were stabilized at 600 °C to test their apatite formation and atomic structure.

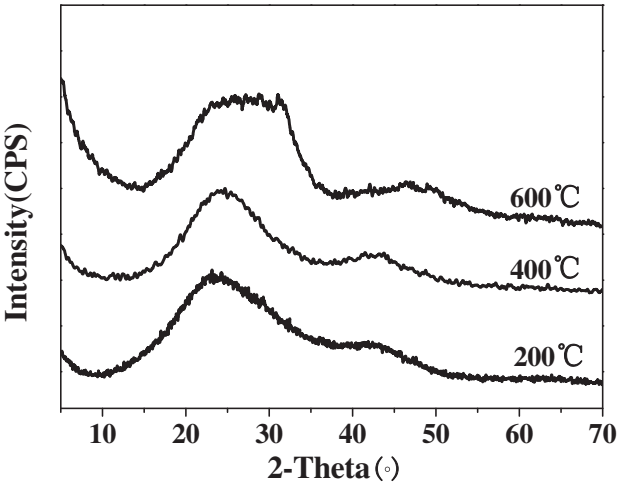


**Fig. 2.** The XRD spectra of PSC glasses after stabilization at 200 °C, 400 °C and 600 °C.

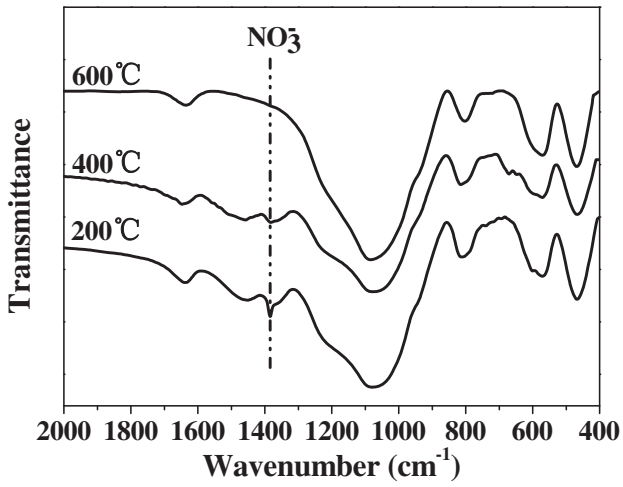


**Fig. 3.** The FTIR spectra of PSC glasses after stabilized at different temperature.

### 3.4. SBF immersion and textural characterization

Apatite formation on the surface of the glasses after immersion in SBF has been a criterion for the *in vitro* bioactivity test [19]. PSC glasses were immersed in SBF for 1 d to test their bioactivity, as shown in Fig. 4. It is found that PSC sample is totally amorphous before SBF immersion, however, the hydroxyapatite diffraction peaks appear for 1 d immersion (Fig. 4a), confirming hydroxyapatite formation on the surface of the sample. For example, the (002) peak at 26°, the (211) peak at 32°, the (212) peak at 40°, the (222) peak at 47°, and the (213) peak at 49°were all observed from the XRD curves, indicating that PSC glass is bioactive. The double peaks at 567 and 603 $cm^{-1}$ are the evidence of phosphate. Fig. 4b show that no phosphate appears for PSC glass before immersion in SBF, whereas, phosphate signals are detected for 1 d immersion, again confirming the formation of hydroxyapatite. In previously, 45S5 and S70C30 glasses have also been reported to form hydroxyapatite for 1 d immersion in SBF [10,26], which means that PSC glass has similar *in vitro* bioactivity with 45S5 and S70C30 glasses. The BET specific surface area (SSA) of PSC, S70C30 and 45S5 glass powders are 121.13 $m^2/g$, 41.27 $m^2/g$ and 0.19 $m^2/g$, respectively, which mean that PSC glass has higher BET surface area than other two composition (45S5 and S70C30).

### 3.5. Characterization of the structure of the samples at the atomic scale

As shown in above, this new PSC glass with higher phosphate content have similar *in vitro* bioactivity with the 45S5 and S70C30 glasses which have lower or no phosphate content. In order to optimize the design of new bioactive glass, the detailed atomic structure of PSC glass was studied comparing with traditional glasses (45S5 and S70C30). HEXRD experiments were carried out to characterize the phosphosilicate networks. The atomic structures of amorphous silicate and phosphate materials had been well characterized by this technique [16,17,27]. The X-ray interference function data is shown in Fig. 5 and the structural parameters for the total diffraction patterns are given in Table 1. Differences are observed for the average separations of Si-O, P-O and Ca-O: PSC has a larger average Si-O and P-O distances and shorter average Ca-O distance than 45S5 and S70C30, implying there might be different silicon and phosphorus coordination environment. However, these differences may be questioned by their uncertainties, indicating the limitation of HEXRD on characterizing the atomic scale structure of such networks with multiple components. Therefore, other complementary spectroscopic techniques should be used as the

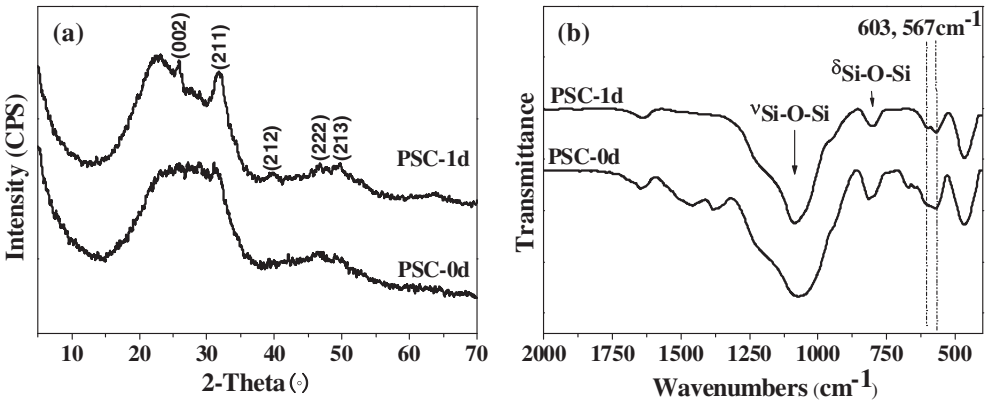


**Fig. 4.** XRD (a) and FTIR (b) spectra of PSC glasses after immersing in SBF for 1 d.

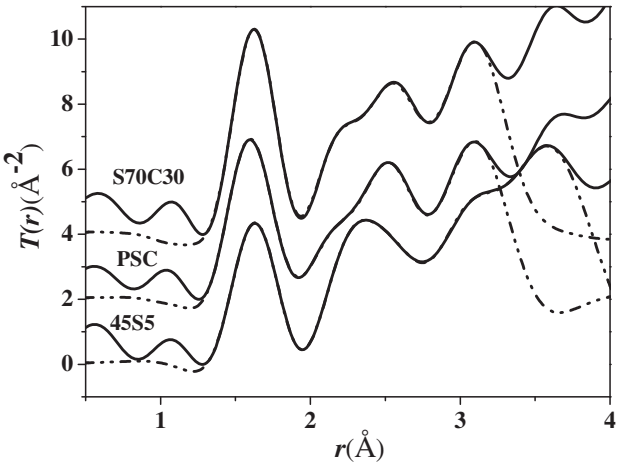


**Fig. 5.** The real-space data X-ray diffraction patterns of 45S5, S70C30 and PSC glasses, as determined from HEXRD data (solid curves: experimental; dashed curves: NXFIT data).

**Table 1**
Structural parameters for the total correlation function T(r).

| | S70C30 | | PSC | | 45S5 | |
|---|---|---|---|---|---|---|
| | *r*(Å) | N | *r*(Å) | N | *r*(Å) | N |
| P-O | – | – | 1.58 | 3.9 | 1.49 | 4.1 |
| Si-O | 1.62 | 4.0 | 1.65 | 4.1 | 1.58 | 4.0 |
| Ca-O | 2.17 | 4.2 | 2.15 | 2.0 | 2.50 | 7.8 |
| O-O | 2.52 | 17.3 | 2.52 | 16.3 | 3.10 | 5.3 |

Typical errors are ± 0.02 Å on the peak position (*r*) and ± 0.2 on the coordination number (N) parameter.

corroborative evidence for the silicon and phosphorus coordination environment.

The solid state $^{31}P$ and $^{29}Si$ MAS NMR were also used to characterize the structure of the phosphosilicate networks of 45S5, S70C30 and PSC glasses, as shown in Fig. 6, the corresponding parameters are shown in Table 2. The connectivity around silicate (phosphate) units is designated using the $Q^n$ ($Q^{n'}$) notation, where n (n′) refers to the number of Si-O-X (P-O-X) bridges around the silicon (phosphorus) center (X = Si, P). For $^{31}P$ MAS NMR, overlapping resonances are observed for PSC sample ($Q^{0'}$, $\delta_{iso}$ (2.0 ppm); and $Q^{1'}$, $\delta_{iso}$ (− 7.3 ppm)), however, only one resonance is observed for 45S5 ($Q^{0'}$, $\delta_{iso}$ (7.7 ppm)), which is essentially isolated $PO_4$ units throughout the structure. For $^{29}Si$ MAS NMR, overlapping resonances are observed for 45S5, S70C30 and PSC glasses. 45S5 samples have a limited connectivity, as mainly $Q^0$ (− 78.5 ppm) and $Q^1$ units (− 84.9 ppm) are present. $Q^1$ (− 88.3 ppm) and $Q^4$ (− 111.6 ppm) units are predominant for S70C30 glasses, indicating an increase in the network connectivity, as expected with higher network former content. Similarly, $Q^3$ (− 104.9 ppm) and $Q^4$ (− 110.4 ppm) units are predominant for PSC glasses, and the resonance become more negative, indicating higher network connectivity (Si-O-Si and P-O-Si). These results give complementary information on the structure of the glasses network, and reveal that there are Si-O-P linkages formed for PSC sample, however, no Si-O-P linkage is formed for 45S5 judged by the sole presence of $Q^0$ phosphorus species. Instead, in 45S5, phosphorous does not enter the network but remains in distinct orthophosphate ($PO_4$, units).

## 4. Discussion

It was reported that the silicate-based glasses degrade slowly and usually take much long time to disappear from the body [11], which may because the higher silica content in glass decreases the rate of dissolution [10]. Given the good biocompatibility and bioresorbability of phosphate materials, increasing $P_2O_5$ content in bioactive materials

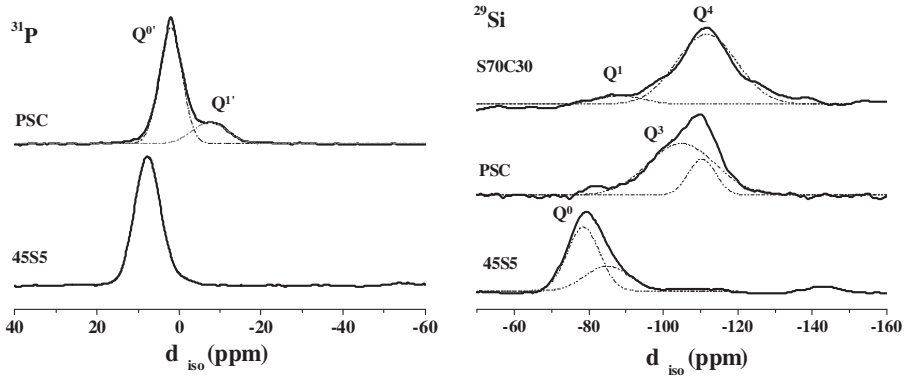


**Fig. 6.** Solid state MAS NMR data for (a) $^{31}P$ spectra and (b) $^{29}Si$ spectra.

**Table 2**
Solid state NMR parameters obtained by de-convolution of the NMR spectra in Fig. 6. (δ: chemical shift; EV: Environment).

| Bioglass | $\delta_{iso}$ (ppm) | EV(%) | $\delta_{iso}$ (ppm) | EV(%) | $\delta_{iso}$ (ppm) | EV(%) | $\delta_{iso}$ (ppm) | EV(%) |
|---|---|---|---|---|---|---|---|---|
| Nucleus | $^{29}$Si | $^{29}$Si | $^{29}$Si | $^{29}$Si | $^{31}$P | $^{31}$P | $^{31}$P | $^{31}$P |
| PSC | − 104.9 | $Q^3$/78 | − 110.4 | $Q^4$/22 | 2.0 | $Q^{0'}$/80 | − 7.3 | $Q^{1'}$/20 |
| 45S5 | − 78.5 | $Q^0$/65 | − 84.9 | $Q^1$/35 | 7.7 | $Q^{0'}$/100 | – | – |
| S70C30 | − 88.3 | $Q^1$/9 | − 111.6 | $Q^4$/91 | – | – | – | – |

certainly has better control on dissolution rates [3]. Therefore, in previous study, we chose phytic acid as phosphorus precursor to produce different composition of bioactive glasses, in which PSC glass composition was found to have the best bioactivity and also have higher phosphate content than conventional glasses [12].

In a recent study, the PSC glass with higher phosphate content was reported to have better cell proliferation, mRNA expression and osteocalcin and mineralization of hDPCs than conventional 45S5 [13], and also have higher ions dissolution rate than 45S5 glass, and S70C30 glass have much higher silicon content than 45S5, thus they may also degrade slowly and usually were prepared as scaffolds to study their *in vitro* and *in vivo* bioactivity [28,29]. The BET specific surface area (SSA) of PSC glass was higher than other two composition (45S5 and S70C30), thus which may also accelerate the degradation rate of PSC glass.

PSC glass with higher phosphate content had similar hydroxyapatite formation with traditional 45S5 and S70C30 glasses with lower or no phosphate content (Fig. 4). Therefore, the detailed atomic structure of PSC glass was studied comparing with traditional glasses (45S5 and S70C30) by HEXRD and NMR techniques (Fig. 5 and Fig. 6). It was clearly shown that PSC glasses have mixed phosphosilicate networks, and the silicates are linked to phosphates (Si-O-P), however, there is no Si-O-P linkage formed for 45S5. And also because of the higher affinity of phytic acid with calcium ions, the calcium ions are in the vicinity of phosphorus units [12,16]. The phosphate ions release may accompany with the calcium ions release during the breakage of Si-O-P linkages of PSC glass in SBF facilitating the formation of hydroxyapatite, illustrating its good *in vitro* bioactivity. Future work will work on the degradation test, ion release, pH value change and cell biocompatibility of PSC glass to see the influence of higher phosphate content.

## 5. Conclusion

A new bioactive glass composition (PSC, $(CaO)_{0.35}(SiO_2)_{0.54}(P_2O_5)_{0.11}$) with higher phosphate content have been characterized in detail by XRD, FTIR, MAS NMR and HEXRD. It was found that the calcium ions could be incorporated into the Si-O-P network even at low temperature (200 °C), and the nitrate ions could be removed fully by heating at 600 °C. It was also found that there was P-O-Si covalent bond formation and lower Ca-O bond length for PSC bioactive glass comparing with other composition (45S5 and S70C30). In addition, the hydroxyapatite could be formed on the surface of the new PSC bioactive glass for only 1 d immersion in SBF, implying its good *in vitro* bioactivity.

## Acknowledgements

This work was supported by NSFC (Project 51603210, 51473004, 81470101 and U1232112) and a Royal Society/Natural Science Foundation of China international exchange grant (IE131323, 51411130151). We acknowledge the help from the station member at the beamline 13W at Shanghai Synchrontron Radiation Facility.

## References

[1] J.R. Jones, Review of bioactive glass: from Hench to hybrids, Acta Biomater. 9 (2013) 4457–4486.
[2] D. Arcos, M. Vallet-Regí, Sol-gel silica-based biomaterials and bone tissue regeneration, Acta Biomater. 6 (2010) 2874–2888.
[3] E.A. Abou Neel, D.M. Pickup, S.P. Valappil, R.J. Newport, J.C. Knowles, Bioactive functional materials: a perspective on phosphate-based glasses, J. Mater. Chem. 19 (2009) 690–701.
[4] F. Baino, G. Novajra, V. Miguez-Pacheco, A.R. Boccaccini, C. Vitale-Brovarone, Bioactive glasses: special applications outside the skeletal system, J. Non-Cryst. Solids 432 (2016) 15–30.
[5] F. Baino, S. Fiorilli, C. Vitale-Brovarone, Bioactive glass-based materials with hierarchical porosity for medical applications: review of recent advances, Acta Biomater. 42 (2016) 18–32.
[6] X. Liu, W. Huang, H. Fu, A. Yao, D. Wang, H. Pan, W.W. Lu, Bioactive borosilicate glass scaffolds: improvement on the strength of glass-based scaffolds for tissue engineering, J. Mater. Sci. Mater. Med. 20 (2009) 365–372.
[7] W. Huang, D.E. Day, K. Kittiratanapiboon, M.N. Rahaman, Kinetics and mechanisms of the conversion of silicate (45S5), borate, and borosilicate glasses to hydroxyapatite in dilute phosphate solutions, J. Mater. Sci. Mater. Med. 17 (2006) 583–596.
[8] L.L. Hench, The story of Bioglass®, J. Mater. Sci. Mater. Med. 17 (2006) 967–978.
[9] J.R. Jones, D.S. Brauer, L. Hupa, D.C. Greenspan, Bioglass and bioactive glasses and their impact on healthcare, Int. J. Appl. Glas. Sci. 7 (2016) 423–434.
[10] P. Saravanapavan, J.R. Jones, S. Verrier, R. Beilby, V.J. Shirtliff, L.L. Hench, J.M. Polak, Binary CaO-$SiO_2$ gel-glasses for biomedical applications, Bio-Med. Mater. Eng. 14 (2004) 467–486.
[11] M. Hamadouche, A. Meunier, D.C. Greenspan, C. Blanchat, J.P. Zhong, G.P.L. Torre, L. Sedel, Long-term *in vivo* bioactivity and degradability of bulk sol-gel bioactive glasses, J. Biomed. Mater. Res. 54 (2001) 560–566.
[12] A. Li, D. Qiu, Phytic acid derived bioactive CaO-$P_2O_5$-$SiO_2$ gel-glasses, J. Mater. Sci. Mater. Med. 22 (2011) 2685–2691.
[13] C. Cui, S. Wang, H. Ren, A. Li, D. Qiu, Y. Gan, Y. Dong, Regeneration of dental-pulp complex-like tissue using phytic acid derived bioactive glasses, RSC Adv. 7 (2017) 22063–22070.
[14] R.A. Martin, H.L. Twyman, G.J. Rees, J.M. Smith, E.R. Barney, M.E. Smith, J.V. Hanna, R.J. Newport, A structural investigation of the alkali metal site distribution within bioactive glass using neutron diffraction and multinuclear solid state NMR, Phys. Chem. Chem. Phys. 14 (2012) 12105–12113.
[15] A. Li, Y. Ma, D. Qiu, Formation of six-coordinated silicon in calcium phosphosilicate xerogels assisted by polyols at low temperature and pressure, Chin. Chem. Lett. 26 (2015) 768–772.
[16] A. Li, D. Wang, J. Xiang, R.J. Newport, M.X. Reinholdt, P.H. Mutin, D. Vantelon, C. Bonhomme, M.E. Smith, D. Laurencin, D. Qiu, Insights into new calcium phosphosilicate xerogels using an advanced characterization methodology, J. Non-Cryst. Solids 357 (2011) 3548–3555.
[17] D.M. Pickup, R.M. Moss, D. Qiu, R.J. Newport, S.P. Valappil, J.C. Knowles, M.E. Smith, Structural characterization by X-ray methods of novel antimicrobial gallium-doped phosphate-based glasses, J. Chem. Phys. 130 (2009) 064708.
[18] Y. Sun, A. Li, H. Ren, X. Zhang, C. Wang, D. Qiu, Removal of residual nitrate ion from bioactive calcium silicate through soaking, Chin. Chem. Lett. 27 (2016) 579–582.
[19] T. Kokubo, H. Takadama, How useful is SBF in predicting in vivo bone bioactivity? Biomaterials 27 (2006) 2907–2915.
[20] A. Li, H. Shen, H. Ren, C. Wang, D. Wu, R.A. Martin, D. Qiu, Bioactive organic/inorganic hybrids with improved mechanical performance, J. Mater. Chem. B 3 (2015) 1379–1390.
[21] C. Wang, Y. Xie, A. Li, H. Shen, D. Wu, D. Qiu, Bioactive nanoparticle through post-modification of colloidal silica, ACS Appl. Mater. Inter. 6 (2014) 4935–4939.
[22] C. Wang, H. Shen, Y. Tian, Y. Xie, A. Li, L. Ji, Z. Niu, D. Wu, D. Qiu, Bioactive nanoparticle-gelatin composite scaffold with mechanical performance comparable to cancellous bones, ACS Appl. Mater. Inter. 6 (2014) 13061–13068.
[23] A.P. Hammersley, S.O. Svensson, M. Hanfland, A.N. Fitch, D. Hausermann, Two-dimensional detector software: from real detector to idealised image or two-theta scan, High Pressure Res. 14 (1996) 235–248.
[24] P. Juhás, T. Davis, C.L. Farrow, S.J.L. Billinge, *PDFgetX3*: a rapid and highly automatable program for processing powder diffraction data into total scattering pair distribution functions, J. Appl. Crystallogr. 46 (2013) 560–566.
[25] S. Lin, C. Ionescu, K.J. Pike, M.E. Smith, J.R. Jones, Nanostructure evolution and calcium distribution in sol-gel derived bioactive glass, J. Mater. Chem. 19 (2009) 1276–1282.
[26] L.L. Hench, Bioceramics: from concept to clinic, J. Am. Cera. Soc. 74 (1991) 1487–1510.
[27] R.A. Martin, H.L. Twyman, G.J. Rees, E.R. Barney, R.M. Moss, J.M. Smith, R.G. Hill, G. Cibin, T. Charpentier, M.E. Smith, J.V. Hanna, R.J. Newport, An examination of the calcium and strontium site distribution in bioactive glasses through isomorphic neutron diffraction, X-ray diffractions, EXAFS and multinuclear solid state NMR, J. Mater. Chem. 22 (2012) 22212–22223.
[28] J.R. Jones, L.M. Ehrenfried, L.L. Hench, Optimising bioactive glass scaffolds for bone tissue engineering, Biomaterials 27 (2006) 964–973.
[29] S. Midha, T. Bo Kim, W. van den Bergh, P.D. Lee, J.R. Jones, Preconditioned 70S30C bioactive glass foams promote osteogenesis *in vivo*, Acta Biomater. 9 (2013) 9169–9182.